DTU Library

Partitioning of ecosystem respiration in a beech forest

Brændholt, Andreas; Ibrom, Andreas; Larsen, Klaus Steenberg; Pilegaard, Kim

[Link back to DTU Orbit](#)

Title

Partitioning of ecosystem respiration in a beech forest

Andreas Brændholt[1*], Andreas Ibrom[1], Klaus Steenberg Larsen[1,2] and Kim Pilegaard[1]

[1]DTU Environment, Technical University of Denmark; [2]Department of Geosciences and Natural Resource Management, University of Copenhagen.

*Correspondence author at: Bygning 115, Bygningstorvet, 2800 Kongens Lyngby, Denmark. E-mail address: andbr@env.dtu.dk

ABSTRACT

Terrestrial ecosystem respiration (R_{eco}) represents a major component of the global carbon cycle. It consists of many sub-components, such as aboveground plant respiration and belowground root and microbial respiration, each of which may respond differently to abiotic factors, and thus to global climate change. To correctly predict future carbon cycles in forest ecosystems, R_{eco} must therefore be partitioned and understood for each of its various components.

In this study we used the eddy covariance technique together with manual and automated closed-chambers to quantify the individual components of R_{eco} in a temperate beech forest at diel, seasonal and annual time scales. R_{eco} was measured by eddy covariance while respiration rates from soil, tree stems and isolated coarse tree roots were measured bi-hourly by an automated closed-chamber system. Soil respiration (R_{soil}) was measured in intact plots, and heterotrophic R_{soil} was measured in trenched plots. Tree stem (R_{stem}) and coarse root (R_{root}) respiration were measured by custom made closed-chambers

24   We found that the contribution of R_{stem} to total R_{eco} varied across the year, by only accounting for 6

25   % of R_{eco} during winter and 16 % during the summer growing season. In contrast R_{soil} was

26   approximately half of R_{eco} during winter (52 %), spring (45 %) and summer (49 %), while the

27   contribution increased to 79 % during autumn.

28   Based on observed fluxes in the trenched and intact soil plots, we found that autotrophic R_{soil}

29   accounted for 34 % of R_{soil} during summer, i.e. a relatively low fractional estimate compared to

30   findings from other studies. It is likely that dead roots were still decomposing in the trenched soil

31   plots thus causing overestimation of heterotrophic R_{soil}.

32   Diel R_{stem} and R_{root} measurements showed a distinct pattern during summer with the highest

33   respiration rates around 13:00-15:00 CET for R_{stem}, and the highest respiration seen from 9:00-15:00

34   for R_{root}. In contrast, R_{soil} showed the lowest respiration during daytime with no clear difference in

35   the diel pattern between the intact and trenched soil plots.

36   Finally, we calculated annual R_{soil} for different transects, and found that annual R_{soil} estimated from

37   the previously used transect at the site was underestimated due to R_{soil} of the transect not being

38   representative for the spatial heterogeneity of R_{soil} at the site. This highlights the importance of

39   performing a sufficient number of chamber measurements at a site to adequately capture the spatial

40   variation and estimate R_{soil} correctly.

41

42   Keywords: Ecosystem respiration, flux partitioning, eddy covariance, chamber, seasonality

43

44   1 Introduction

45   Ecosystem respiration (R_{eco}) is, after gross primary productivity (GPP), the second largest flux of

46   CO_2 between the biosphere and the atmosphere (Beer et al. 2010; IPCC, 2013). R_{eco} is the sum of

47   respiration from several component of the ecosystem that may respond differently to abiotic factors,

and thus to global change (Schimel et al., 2001; Valentini et al., 2003). To correctly understand and predict future ecosystem carbon cycles, R_{eco} must therefore be partitioned into its main sub-components. For forests, major components are aboveground autotrophic respiration from the leaves, branches and stems of the trees, and belowground by the autotrophic respiration from tree roots and the heterotrophic respiration from soil microbes, which together form the soil respiration (R_{soil}) (Hanson et al., 2000; Högberg et al. 2005, Rodeghiero and Cescatti, 2006).

Ecosystem-level net atmospheric exchange of CO_2 (NEE) can be measured on a high temporal scale by the eddy covariance method (e.g. Pilegaard et al., 2001; Wofsy et al., 1993). NEE can be partitioned into GPP and R_{eco}, by various extrapolation methods, one of which uses temperature response functions to extrapolate from measured nighttime respiration rates to estimates of daytime respiration (Reichstein et al., 2005). Whereas eddy covariance provides R_{eco} on a high temporal scale, it does not provide information on the individual components that make up R_{eco}. Instead, chamber based methods can be used to measure the CO_2 flux from the individual components by enclosing a specific part of the ecosystem in a chamber. Typically, chambers of the closed type are used, where the CO_2 flux is calculated based on the near-linear increase in chamber CO_2 concentration during the measurement. Chamber-based methods differ from the eddy covariance method by the smaller spatial coverage (Wang et al., 2010). Eddy covariance covers a large footprint area that may be representative for the studied ecosystem (Nagy et al., 2006). R_{soil}, however, often show a high degree of spatial heterogeneity within the footprint area (Knohl et al., 2008; Webster et al., 2008). At eddy covariance sites, R_{soil} is often determined with manually operated soil chambers (e.g. Wu et al., 2013). To ensure that R_{soil} measurements are representative for the eddy covariance footprint, a sufficient number of measurements must be performed throughout the footprint (Davidson et al., 2002; Savage et al., 2008). By performing the manual chamber measurements distributed throughout the footprint at regular intervals throughout the year,

3

72 both the seasonal change in R_{soil} and the spatial difference in R_{soil} can be captured to give a good

73 estimate of R_{soil} for the footprint (Savage and Davidson, 2003). However, because of labour

74 intensiveness, manual measurement campaigns rarely capture diel or day to day variability in the

75 fluxes. Automated chamber systems can allow for measurements at much higher temporal

76 resolution, but because of budget constraints usually only a limited number of automated chambers

77 are available causing low spatial coverage of automatic systems. Apart from R_{soil}, measurements of

78 other ecosystem components such as respiration from leaves, branches and tree stems and woody

79 debris lying on the soil surface have been made using both manual and automated chambers

80 (Rodríguez-Calcerrada et al., 2014; Tang et al., 2008; Zhu et al., 2012). As for R_{soil}, these

81 components can show a high degree of spatial and temporal variability throughout the footprint,

82 thus requiring a sufficient number of chamber measurements to capture this variability.

83 The diel pattern of R_{soil} is generally related to soil temperature (Janssens and Pilegard, 2003; Tang

84 et al., 2005). However, differences in substrate input of carbon from photosynthesis to the soil via

85 the roots can vary across the day (Kuzyakov and Gavrichkova, 2010). Diel changes in substrate

86 input from plants may completely or partly decouple R_{soil} from the diel pattern of soil temperature

87 (Tang et al., 2005). To study the influence of substrate input and the autotrophic contribution from

88 roots to R_{soil}, a trenching can be performed. Here the contribution of roots to R_{soil} is removed by

89 cutting off any roots in a plot and preventing them to grow back (Baggs, 2006; Bond-Lamberty et

90 al., 2011). This stops autotrophic R_{soil} and prevents any input of carbon from photosynthesis.

91 However, the roots are left to decay in the plot and the soil water content may increase (Díaz-Pinés

92 et al., 2010). By comparing plots with intact soil to plots with trenched soil, the heterotrophic and

93 autotrophic components of R_{soil} can be investigated.

94 The aim of the study was to quantify the CO_2 fluxes from various components of a forest ecosystem

95 on an annual, seasonal, daily and diel scale, and to quantify how the contribution to total R_{eco} of

heterotrophic and autotrophic R_{soil} and stem respiration (R_{stem}) vary on a seasonal scale. This was achieved by a combination of the eddy covariance method and manual and automated closed-chamber techniques.

2 Materials and Methods

2.1 Site description

Measurements were performed at the Danish ICOS RI site called DK-Sor at 40 m a.s.l. (55°29'13'' N, 55°38''45'' E), where eddy covariance measurements of net ecosystem CO_2 fluxes have been performed continuously since 1996. The climate is temperate maritime with an annual average precipitation and an annual average temperature of 564 mm and 8.5 °C, respectively (Pilegaard et al. 2011).

The forest is dominated by European beech (*Fagus sylvatica* L.) planted in 1921 with small stands of Norway spruce (*Picea abies* (L.) Karst) and European larch (*Larix decidua* Mill.) (Wu et al. 2013). The tree stem density is 288 per hectare with an average tree height of 28 m and an average diameter at breast height (DBH) of 42 cm in 2010. The main rooting depth is 1 m (Pilegaard et al. 2011). However, roots are most frequent at a depth of 0-20 cm (Østergård, 2001). The dense canopy has a peak LAI of 5.0 and the average annual canopy cover duration period is 180 days. The understory is poorly developed due to the well-developed canopy, causing a sparsely vegetated forest floor during most of the year, except during spring when wood anemones (*Anemone nemorosa* L.) are present in part of the forest floor. Depending on the base saturation, the soils are classified as either alfisols or mollisols. The soil carbon pool is 20 kg m^{-2} down to 1 m depth, with a C/N ratio of 20 in the upper organic soil layers, decreasing to 10 in the lower mineral layers (Østergård, 2001). The organic layer is 10–40 cm deep (Pilegaard et al. 2001).

2.2 Eddy covariance measurements

120 Measurements of NEE were performed at a height of 43 m on the flux tower on the site by a closed-

121 path eddy covariance system based on a Gill HS-50 3D research sonic anemometer (Gill

122 Instruments Limited, Lymington, UK) and a fast response infrared gas analyser LI-7000 (LI-COR

123 Environmental, Lincoln, Nebraska, USA). For details on the raw data processing, see Pilegaard et

124 al. (2011). Nighttime fluxes at insufficient turbulent mixing were removed when the friction

125 velocity (u_*) was lower than 0.1 m s^{-1} and the atmospheric stratification was stable. A dead band of

126 2 hours after re-establishment of turbulent conditions was applied to avoid double accounting from

127 measuring CO_2 fluxes from venting the canopy air space. The removal of data below the u_*

128 threshold value, and periods of system failure, resulted in a data coverage of 54.1 % for 2016. The

129 data set was gap-filled and NEE was partitioned into GPP and R_{eco} by the online "REddyProc: Eddy

130 covariance data processing tool" (Department of Biogeochemical Integration, MPI Jena). In short,

131 the gap-filling procedure follows the approach by Reichstein et al. (2005), and the partitioning of

132 NEE follows the look-up table approach by Reichstein et al. (2005) and the regression approach by

133 Lasslop et al. (2010). This resulted in a continuous data set of half-hourly values of NEE, GPP and

134 R_{eco} for the entire year. From the half-hourly values, the mean daily values were calculated as well

135 as monthly and annual sums of NEE, GPP and R_{eco}.

136 For the each of the annual sums of NEE, GPP and R_{eco} an uncertainty estimate was calculated. Wu

137 et al. (2013) used five years of data to calculate the relative uncertainties of the annual sums of

138 NEE, GPP and R_{eco} for the DK-Sor site by taking the uncertainties caused by u_* filtering, gapfilling

139 and site heterogeneity into account. By using these relative uncertainties, we calculated the

140 uncertainty estimates for the annual sums of NEE, GPP and R_{eco}.

141

142 **2.3 Manual closed-chamber soil respiration measurements**

143 R_{soil} was measured manually using a portable 8100-102 10 cm survey chamber connected to a LI-

144 8100A Automated Soil CO_2 Flux System (LI-COR Environmental, Lincoln, Nebraska, USA). R_{soil}

145 was measured on permanently installed soil collars, inserted 4 cm into the soil, on three distinct

146 transects in the footprint area of the eddy covariance measurements. The R_{soil} plots contained litter

147 but no living plants. The first transect, called the inside fence transect, consisted of 12 plots that

148 were positioned within 15 m of the flux tower. The second transect, called the south transect,

149 consisted of 27 plots, which were positioned at 9 locations along a straight line starting 30 m from

150 the flux tower and ending 270 m south of the tower. Each of the 9 locations contained 3 R_{soil} plots.

151 The last transect, called the west transect, consisted of 45 plots. The plots were positioned in groups

152 of three at 15 locations along two parallel lines that were separated by 30 meters. The lines started

153 30 m from the flux tower and ended 210 m to the west. The location for the south and west transects

154 were chosen to be in the main wind directions and source area for the eddy covariance

155 measurement. See Pilegaard et al. (2011) and Wu et al. (2013) for information about the footprint

156 area and wind direction at the site.

157 The manual measurements were performed at an interval of two to three weeks, where R_{soil} was

158 measured once per plot with a chamber closure time of 150 seconds. This resulted in 20 campaign

159 measurements evenly distributed in time during 2016 for each of the transects. The measurements

160 of the three transects were typically performed on two adjacent days between 09:00–16:00 CET,

161 with the inside fence and south transect being measured on the first day, and the west transect being

162 measured on the second day.

163

164 **2.4 Automated closed-chamber measurements**

165 In addition to the manual chamber measurements, automated closed-chamber measurements of

166 respiration from intact soil, trenched soil, coarse roots and tree stems were performed from 4

167 January 2016 to 31 December 2016 with a LI-8100A Automated Soil CO_2 Flux System connected

168 to a LI-8150 Multiplexer (LI-COR Environmental, Lincoln, Nebraska, USA). All the automated

169 soil, root and stem chambers were positioned within 15 m from the flux tower. The system

170 performed well through the entire measurement period leading to automatic measurement being

171 performed each day.

172 R_{soil} was measured by six opaque soil chambers on circular soil collars with a diameter of 20 cm

173 that were permanently inserted 4 cm into the soil. The soil collars contained soil and litter but no

174 aboveground plant parts. One of the soil chambers was an 8100-101 Long-Term CO_2 flux

175 chambers, and five were 8100-104 Long-Term CO_2 flux chambers (LI-COR Environmental,

176 Lincoln, Nebraska, USA). For two of the soil chambers, trenching was first performed on 6 April

177 2016 to remove the contribution of living roots to the total R_{soil} from the plot. The trenching was

178 done by vertically inserting a spade 25 cm into the soil in a circle around the soil chambers. Roots

179 with a diameter too big to be cut with the spade were cut with a saw. To prevent ingrowth of roots,

180 monthly re-trenching was performed throughout the study period. Thus, the six soil chamber plots

181 consisted of two trenched soil plots and four intact soil plots.

182 R_{stem} and R_{root} were measured with two custom made coarse root chambers and two custom made

183 stem chambers, respectively. Unlike the LI-COR soil chambers, the root and stem chambers did not

184 open between measurements. Instead, the chamber headspace was continuously flushed between

185 measurements with atmospheric air that was let into the chamber by a small tube. The flow of air to

186 all root and stem chambers was provided by a pump, and the flow to each chamber set to 1 L min^{-1}

187 by a flow meter. This resulted in a near ambient atmospheric air CO_2 concentration in the chambers

188 between measurements. At the beginning of a chamber measurement, the flow of air to the specific

189 chamber was stopped by automatically closing a normally open solenoid valve that was placed on

190 the flush tube going to the chamber. Thus, the chambers were closed during measurements.

191   The two root chambers were made of transparent acrylic glass and were cylindrical in shape with an

192   inner length of 24 cm and an inner diameter of 7 cm giving a volume of 923 cm^3. Before assembly

193   the cylinder was cut in two halves in the longitudinal axis. A 10 cm long tube with an inner

194   diameter of 0.5 cm, and a filter in the end was attached to the chamber, which acted as a vent to the

195   atmosphere. The chambers were installed in June 2015. For each chamber a suitable coarse root

196   from a soil depth of 5-10 cm was carefully exposed, and the root was rinsed by tap water. The

197   diameter of root was measured, and the root volume and root surface area was calculated. The root

198   was placed in the one half of the cylinder and the other half of the cylinder was placed on top. In

199   each end of the cylinder, the root went through a hole. The two half cylinders were sealed to each

200   other and the hole around the root in each end was sealed with Blu-tack. Following this, the

201   chamber was covered with soil.

202   The two stem chambers were cylindrical and made of polypropylene, with an inner diameter of 15

203   cm and an inner height of 10 cm, giving a volume of 1757 cm^2. A 10 cm vent tube with an inner

204   diameter of 0.5 cm, and a filter in the end was attached at the bottom of the chamber. The chambers

205   were attached to the smooth stem surfaces of two beech trees at a height of 1.3 m by a rubber

206   extrusion with a u-profile that was attached to the chamber and sealed with silicone. The chamber

207   was held in place on the stem by adjustable straps.

208   The ten chambers were connected to the LI-8100A/ LI-8150 in a multiplexed setup, and the system

209   was set up in a repeated automated two-hour cycle during which a measurement of each of the soil,

210   root and stem chambers was performed. The chamber closure time was set to 5 minutes and the pre-

211   purge and post-purge times were set to 40 seconds for all chambers.

212

213   **2.5 Chamber flux calculation and up-scaling of fluxes**

214   All data analysis of the chamber based CO_2 fluxes and post-processing of the eddy covariance data

215   was done using R version 3.2.0 (R Core Team, 2014).

216   CO_2 fluxes for all chamber measurements were calculated for each individual measurement on a

217   time and area basis by fitting the non-linear equation by Hutchinson and Mosier (1981) with the

218   nlsLM function (minpack.lm package) for model fitting in R (Elzhov et al. 2015). For the manual

219   chamber measurements, the first 20 seconds after chamber closure were discarded from the flux

220   calculation (the dead band), whereas the dead band was set to 100 seconds for the automated

221   chamber measurements because an external analyser (used in another study) was attached in

222   parallel with the LI-8100/LI-8150 system, causing increased system volume and therefore increased

223   system response time.

224   The calculated automated chamber fluxes from soil, stem and coarse roots were quality flagged first

225   by removing fluxes with an $r^2 < 0.80$ of the fit. Following this, the automated soil fluxes, but not

226   stem and root fluxes, were further quality flagged by removing measurements performed at low u_*,

227   where soil fluxes measured by the LI-8100A/LI-8150 system at the site have been found to be

228   overestimated (Brændholt et al. 2017). In short, the automated soil chamber fluxes were compared

229   with u_* measured at the flux tower. From a plot of the fluxes against u_*, a threshold value of 0.2 m

230   s^{-1} was determined visually, as where the decrease of fluxes in response to an increase in u_* levelled

231   off. Fluxes below the u_* threshold value were removed from further analysis. In total the quality

232   control removed 16.3 % of the automated root and stem chamber measurements and 44.9 % of the

233   automated soil chamber measurements, leaving 30124 automated chamber measurements for

234   further analysis. For the manual chamber measurements no quality control was applied in the post

235   processing. Instead the quality control was done in the field following a measurement. If the

236   coefficient of variance of the flux, provided by the LI-COR software, was higher than 1.4 %, the

237   measurement was discarded and an extra measurement was performed on the plot.

238   From the quality controlled flux chamber measurements different estimates for the annual CO_2

239   fluxes were calculated for both the manual and automated measurements following the procedure

240   described by Brændholt et al. (2017). For the manual measurements, annual soil CO_2 fluxes were

241   calculated both for the inside fence transect, the south transect and the west transect.

242   For each transect, the manual fluxes were used to parameterize an empirical model of R_{soil} as a

243   function of soil temperature as described by Lloyd and Taylor (1994):

244

245    $$R_s = R_{283} \exp\left[-E_0\left(\frac{1}{T_s+273.15-T_0} - \frac{1}{T_s-T_0}\right)\right],$$ (1)

246

247   where T_0 and E_0 are fitted parameters, T_s is soil temperature measured at 5 cm depth and R_{283} is the

248   base respiration at a soil temperature of 10 °C. The model was fitted with nlsLM in the R package

249   minpack.lm (Elzhov et al. 2015) that uses a nonlinear least squares regression based on a

250   Levenberg–Marquardt algorithm. By using soil temperature at 5 cm depth measured continuously at

251   the site as model driver input, a continuous one-year time series of mean daily R_{soil} was calculated.

252   A potential soil temperature bias could occur if the soil temperature continuously measured inside

253   the fence at the site, which was used for modelling of the annual CO_2 fluxes, systematically differed

254   from the soil temperatures of the manually measured soil respiration plots. However, no systematic

255   soil temperature difference was found, e.g. exemplified by a mean annual soil temperature inside

256   the fence of 8.4 °C compared to mean annual soil temperatures of 8.7 and 8.2 °C for the south

257   transect and west transect, respectively.

258   For the automated measurements, annual mean CO_2 fluxes were calculated for the four intact soil

259   plots, the two trenched soil plots, the two root plots and the two stem plots, respectively. Each of

260   the annual CO_2 fluxes was calculated by first averaging the bi-hourly fluxes on a monthly basis,

261   providing a diel pattern of fluxes for each month. From this, a daily mean flux was calculated on a

262   monthly basis at the average of the bi-hourly values. Monthly fluxes were calculated as the sum of

263   the daily soil fluxes in the respective month, and the annual flux was calculated as the sum of the 12

264   months.

265   The uncertainties of the annual soil CO_2 fluxes based on the manual chamber for each of the three

266   transects were estimated by the approach used in Wu et al. (2013), which is based on Van Oijen et

267   al., (2005). In short, for each transect a Bayesian calibration was used to quantify the uncertainty of

268   the model predictions, for which a Markov Chain Monte Carlo (MCMC) Metropolis-Hastings

269   random walk algorithm was used. We performed 50000 MCMC iterations from which the prior

270   parameter distributions were sampled. Different annual soil CO_2 fluxes were calculated using the

271   estimated posterior parameter distributions, and the standard deviation of the annual soil CO_2 fluxes

272   was interpreted as the uncertainty of the annual soil CO_2 flux for a given transect.

273   R_{stem}, calculated on a stem surface area, was scaled up to the soil surface area by using site data on

274   tree density, tree height and DBH. The tree height and DBH were measured for 54 beech trees

275   during March 2017. For each of the measured trees, the surface stem area was calculated as the

276   surface area of a cylinder with the measured height and a diameter of 0.71 times the measured

277   DBH. This diameter was derived from a form factor for European beech that describes the

278   relationship between the stem ground area at breast height and the volume of wood contained in the

279   stem and branches above a diameter of 5 cm (Landesverwaltungsamt Sachsen-Anhalt). The average

280   stem surface area calculated from the sampled trees was multiplied with the tree density of 288

281   stems ha^{-1} to get the stem surface area scaled on a soil surface area. From this the measured R_{stem} on

282   a stem surface area could be converted to a CO_2 flux on a soil surface area.

283   The uncertainties of the annual soil CO_2 fluxes for the intact soil, trenched and stem measured by

284   the automated chamber were estimated by formal error propagation that took the uncertainties of the

285   various steps in the calculation of the annual fluxes into account. For the annual stem flux, an extra

286 level of uncertainty was included in the calculation that accounted for the uncertainty of the up-

287 scaling of the fluxes from stem surface area to soil surface area. For this, we assumed an uncertainty

288 of 30 % in the stem surface area calculated from the measurements of tree height and DBH.

289

3 Results

3.1 Annual CO_2 budgets

292 Different annual CO_2 budgets were calculated for different components of the forest from both the

293 tower based eddy covariance and the automated and manual closed-chamber measurements.

294 The gap-filled annual NEE calculated from the eddy covariance measurement at a height at 43 m on

295 the flux tower was -391 ± 63 g C m^{-2} yr^{-1}, and the estimated GPP and R_{eco} were 2272 ± 136 and

296 1882 ± 301 g C m^{-2} yr^{-1}, respectively (Fig. 1).

297 Different estimates of annual R_{soil} were calculated based on the manual closed-chamber

298 measurements that were used to parameterize the Lloyd and Taylor model (Fig. 1). The lowest

299 annual R_{soil} of 794 ± 51 g C m^{-2} yr^{-1} was found for the inside fence transect, where the plots were

300 positioned within a distance of 15 m from the eddy flux tower. The annual R_{soil} from the two

301 transects, with soil plots distributed in the forest, were both higher with an annual R_{soil} of 1024 ± 89

302 g C m^{-2} yr^{-1} for the west transect and an annual R_{soil} of 972 ± 90 g C m^{-2} yr^{-1} for the south transect.

303 The average annual R_{soil} based on the automated closed-chamber measurements every two hours

304 was 597 ± 93 g C m^{-2} yr^{-1} for the four automated chambers with intact soil and, while the average

305 annual R_{soil} for the two automated chambers containing trenched soil was 375 ± 29 g C m^{-2} yr^{-1},

306 accounting for 63 % of R_{soil} for the intact soil plots.

307 The annual up-scaled stem CO_2 on a soil surface area basis was 264 ± 88 and 191 ± 64 g C m^{-2} yr^{-1}

308 for the two automated stem chambers, respectively, resulting in an average of 227 ± 108 g C m^{-2} yr^{-}

309 ^{1} (Fig. 1). This was equivalent to 258 ± 15 g C m^{-2} yr^{-1} on a stem surface area basis.

310 Compared to the annual estimate of R_{eco} from the eddy covariance measurements, the annual R_{soil}

311 constituted 43, 55 and 52 % from the manually measured inside fence transect, the west transect and

312 the south transect, respectively, while the annual R_{soil} based in the intact soil plots and trenched soil

313 plots measured automatically constituted 32 and 20 % of R_{eco}, respectively. The average stem CO_2

314 flux constituted 12 % of R_{eco}.

315

316 **3.2 Seasonal forest respiration**

317 R_{eco}, R_{soil} and R_{stem} generally followed the same pattern throughout the year with the lowest

318 respiration rates during the cold winter months and the highest rates during the warm summer

319 months (Fig. 2, Fig. 3). However, the individual contribution of R_{soil} and R_{stem} to the total R_{eco}

320 differed between the seasons. R_{stem} showed a high seasonality in its contribution to the total R_{eco}

321 contributing only 6 % of R_{eco} during the winter months of January, February and December. A

322 similar low contribution of 7 % was seen during the spring months of March, April and May.

323 However, during the summer months of June, July and August the contribution of R_{stem} increased to

324 16 %. In the autumn months of September, October and November the contribution gradually

325 decreased from 16 % in September to a level of 9 % in November, close to the winter level. The

326 monthly pattern of contribution of R_{soil} to the total R_{eco} differed from R_{stem}. Here winter, spring and

327 summer were fairly similar contributing 52, 45 and 49 % to R_{eco}, respectively. However, R_{soil} during

328 the autumn months differed from the rest of the year by contributing 79 % to the total R_{eco}.

329 R_{root}, which was measured for two coarse roots, was not scaled up to the soil surface area because of

330 the various contributions of roots of different sizes to total root respiration.

331

332 **3.3 Effect of trenching**

14

The annual average R_{soil} for the two trenched soil plots measured by the automated chambers was 63 % of annual average R_{soil} for the four intact soil plots. However, the trenching was not performed until 5 April 2016. To investigate the effect of the trenching on R_{soil}, we looked at R_{soil} before and after the trenching. Before the trenching R_{soil} of the trenched plots was 77 % of the R_{soil} for the intact soil. However, for the remaining part of the year following the trenching, R_{soil} for the trenched plots decreased to 61 % of the intact soil plots.

The course of R_{soil} generally followed the same pattern throughout the year for both the intact and trenched soil plots, by following changes in soil temperature (Fig. 3). However, during the months of June, July and August where GPP was highest (Fig. 4), the intact soil plots reached higher levels of R_{soil} with R_{soil} of the trenched soil plots only being 51 % of the intact plots. R_{soil} of one of the intact soil plots differed by showing a rapid increase in R_{soil} during April and May, but then decreasing again to a level similar to the remaining intact soil plots (Fig. 3). For October, November and December during autumn and winter, where GPP was low to near zero μmol m^{-2} s^{-1}, R_{soil} of the intact soil plots decreased to almost the level of the trenched soil plots, with R_{soil} of the trenched plots being 83 % of the intact plot, a higher level than the pre-trenching level of 77 %.

3.4 Stem respiration and GPP

A rapid increase in GPP was seen in May following the leaf out of the deciduous beech trees (Fig. 4). GPP peaked in June and the high GPP continued into July, following by lower GPP in August and September. A similar rapid increase in May was not seen for the two R_{stem} plots. Instead, a slower increase was seen in May followed by a peak in R_{stem} in July and August. During autumn, however, the decrease in R_{stem} did seem to follow the decrease in GPP. Instead of following GPP, the course of R_{stem} followed the course of R_{soil} during spring, summer and autumn (Fig. 4). However, during summer a higher day to day variability was seen for R_{soil} compared to R_{stem}.

15

357

3.5 Diel patterns of CO₂ fluxes

The automated chamber measurements performed every two hours throughout the year allowed for investigating the diel patterns of R_{stem}, R_{root} and R_{soil} for both the trenched and intact soil plots for the different seasons of the year (Fig. 5).

Although R_{soil} was higher for the intact soil plots than for the trenched plots, the diel pattern of R_{soil} generally exhibited the same pattern for both the intact (Fig. 5a, b, c, d) and the trenched soil plots (Fig. 5a, b, c, d). During winter, R_{soil} was generally higher during daytime than during nighttime. For spring and autumn, however, no clear diel pattern was observed. Summer exhibited a diel pattern with generally low R_{soil} during daytime. A peak in R_{soil} was seen early in the morning and late in the evening before midnight. The diel patterns of R_{stem} and R_{root} during summer differed from R_{soil} by having the highest respiration rates during daytime (Fig. 5k, o). R_{stem} peaked at 13:00-15:00 CET, while a longer peak period from 9:00-15:00 was seen for R_{root}. For winter and autumn, no diel pattern was seen for R_{root} (Fig. 5i, l). However, during spring, a similar diel pattern as during summer with highest R_{root} during daytime was observed. The diel pattern of R_{stem} during spring and autumn was similar to the diel pattern during summer, although less pronounced, with highest R_{stem} during daytime. R_{stem} for winter, however, showed no diel pattern, which was in contrast to the high daytime R_{stem} seen during the rest of the year.

Soil temperature at 5 cm depth generally showed no diel pattern during winter, summer and autumn (Fig. 6). During spring, however, a moderate diel pattern was observed with highest soil temperatures late in the afternoon or early in the evening and the lowest soil temperatures in the morning. The difference between the highest and lowest diel temperature was, however, only approximately 1 °C.

17

4 Discussion

4.1 Annual R_{soil} at different transects

We measured R_{soil} at three different transects, which revealed that the annual R_{soil} measured on the inside fence transect was 20 % lower than the average annual R_{soil} measured on the west and south transects. Manual R_{soil} measurements on the inside fence transect have previously been used on the site to estimate annual R_{soil}. Wu et al. 2013 found an average annual R_{soil} of 752 ± 30 g C m^{-2} yr^{-1} for a 5 year period, which is close to the 794 ± 51 found in this study. They calculated the aboveground autotrophic respiration to 872 g C m^{-2} yr^{-1}, which they found to be unexpectedly high. They argued that it could be explained if R_{soil} had been underestimated, due to the plots having lower R_{soil} than the average R_{soil} of the footprint. The inside fence transect consisted of 12 plots all positioned within 15 meter of the flux tower, at a relatively dry and high ground. In contrast, the two newly established west and south transects, not used in Wu et al. (2013), consisted of 27 and 45 plots, respectively, that were spread out evenly in the forest. R_{soil} and soil moisture measured at both transects showed a higher variation than R_{soil} and soil moisture measured at the inside fence transect (Data not shown). Thus, we argue that the two new transects better represent the spatial variation of R_{soil} in the eddy covariance footprint than the inside fence transect. The annual R_{soil} for the two transects were, however, also similar (972 ± 90 and 1024 ± 89 g C m^{-2} yr^{-1}), constituting 53 % of R_{eco}. Knohl et al. (2008) recommended using at least 8 measurement locations spaced randomly throughout the area of interest to get a representative estimate of R_{soil} with sufficient confidence. The two new transects contained 9 and 15 locations throughout the eddy covariance footprint, respectively, each location containing 3 soil collars. Thus, measuring R_{soil} on only one of these transects might be sufficient to cover the spatial variability and get a solid estimation of R_{soil}. The minor difference between the annual R_{soil} from the two transects also supports this. In contrast, the

18

404   12 soil collars in the inside fence transect only cover 1 location because they are placed closely

405   together, and therefore do not live up to the recommendations by Knohl et al. (2008).

406   If the new transects had been used in Wu et al. (2013), the higher R_{soil} would have changed the

407   extremely high estimate of aboveground autotrophic respiration. If we correct R_{soil} in Wu et al.

408   based on the relationship between R_{soil} of the inside fence transect and the other two transects in this

409   study, then the annual R_{soil} increases from 752 to 945 C m^{-2} yr^{-1}. This is turn would lower the

410   estimate of aboveground autotrophic respiration from 872 to 679 g C m^{-2} yr^{-1}, and make the

411   estimates of above and belowground autotrophic respiration more similar as would be expected

412   (Wu et al. 2013).

413   The annual R_{soil} based on the automated closed-chamber measurements on the 4 intact soil plots was

414   597 ± 93 g C m^{-2} yr^{-1}, lower than annual R_{soil} of the 3 transects measured by manual chambers. The

415   automated measurements were performed within 15 m from the flux tower, close to the 12 plots of

416   the inside fence transect. Thus, a somewhat similar annual R_{soil} could be expected. However, the

417   annual R_{soil} of the inside transect was 794 ± 51 g C m^{-2} yr^{-1}, higher than the annual R_{soil} based on the

418   automated measurements. The cause for the difference in R_{soil} is unknown. Even though the plots

419   are positioned close to each other, it is possible that spatial heterogeneity within a few metres have

420   caused the difference in R_{soil}. Another possibility is the different closed-chamber systems used, that

421   potentially could lead to different absolute flux values. Lastly, it is possible that the difference

422   between the day time only measurements for the manual chambers and the measurements every two

423   hours for the automated chambers have caused the difference in R_{soil}.

424

425   **4.2 Comparison of annual respiration**

426   GPP was found to be 2272 ± 136 g C m^{-2} yr^{-1} (Fig. 1). This is high compared to the average of 1881

427   ± 127 g C m^{-2} yr^{-1} that has previously been found for the site (Wu et al. 2013). We expect an

optimal growing season during the study period to be part of the reason for this. No summer

drought was observed, which has been found to lower forest growth during summer, thus lowering

annual GPP (Ciais et al., 2005). The trees could therefore continue to photosynthesize without any

edaphic or climatic reduction during summer. Furthermore, September was exceptionally warm,

which allowed the trees to continue photosynthesizing for an additional period at high rates (Fig. 4).

R_{eco} was found to be high as well at 1882 ± 301 g C m^{-2} yr^{-1}, which is to be expected due to the

commonly found link between GPP and R_{eco} (Mahecha et al., 2010; Peichl et al., 2013) and higher

than the 1624 ± 201 g C m^{-2} yr^{-1} found by Wu et al. (2013). Luyssaert et al. (2007) assembled a

global database of GPP and R_{eco} and reported the average GPP and R_{eco} to be 1375 ± 56 and $1048 \pm$

64, respectively, for temperate humid deciduous forests, which is much lower than found for the

DK-Sor forest. However, we expect GPP and R_{eco} for the DK-Sor forest to be higher because the

forest is at its main productive phase with a uniform stand of 100 year-old beech trees with high

LAI and a fertile soil. Furthermore, the mild maritime climate and the moderately high latitude

close to the northern margin of beech forest's geographic range have relatively long days during the

vegetation period. With a canopy process model, Ibrom et al. (2006) showed for two different

conifer canopies that the northern, maritime climate in Scotland increased the photosynthetically

active radiation use efficiency by 13-14 % compared to a more continental climate at a forest site in

Central Germany. The reason was longer day lengths, a higher fraction of diffuse radiation and

lower vapour pressure deficit at the Scottish site. Compared to the main beech distribution area with

many drier and more continental sites, we conclude that the site conditions at the DK-Sor beech

forest site allow for comparably high forest productivity.

We found an average annual R_{stem} per unit ground area of 227 ± 108 g C m^{-2} yr^{-1}, which is the first

estimate for this flux component at this site (Fig. 1). The quantification of the CO_2 flux from tree

stems has not received the same attention as e.g. R_{soil} and R_{eco}, probably associated with the extra

452   work and cost required to construct and operate the custom made stem chambers, and the

453   complications to upscale the measurements to the total stand level. R_{stem} can, however, be a

454   substantial part of R_{eco}, and constituted 12 % of R_{eco} in our study. A few studies have addressed the

455   role of R_{stem} for different forest ecosystems (Ceschia et al., 2002; Edwards and Hanson, 1996;

456   Inoue, 2004; Saveyn et al., 2007; Yang et al., 2015; Zha et al., 2004), and a few studies have looked

457   at R_{stem} for beech trees (Ceschia et al., 2002; Damesin et al., 2012; Saveyn et al., 2007). Tang et al.

458   (2008) found that R_{stem} accounted for 13 % of R_{eco} in a temperate old-growth hardwood forest in the

459   USA, close to the findings for our forest. Damesin et al. (2002) measured respiration from stem and

460   branches and estimated the annual respiration to be between 325 and 383 g C m^{-2} yr^{-1}, with R_{stem}

461   accounting for approximately 50 %. In a review of 18 European forests, Janssens et al. (2000) found

462   that aboveground respiration accounted for 31 % of R_{eco}. If half of the aboveground respiration is

463   accounted for by R_{stem} as found by Damesin et al. (2002), then 12 % of R_{eco} accounted for by R_{stem} in

464   our study is close to the findings by Janssens et al. (2000).

465   Upscaling R_{stem} from chamber based measurements to soil surface area for comparison with other

466   ecosystem respiration components can cause considerable up-scaling biases. Three main causes of

467   errors can be identified: Insufficient number of measurements in time to catch the temporal

468   resolution in R_{stem}, insufficient number of measurements to catch the spatial variability in R_{stem}

469   between and within trees, and uncertainty related to scaling up surface measurements to the entire

470   surface of the tree stand. The automatic stem chambers ran continuously throughout the year, thus

471   capturing even the hourly variation of R_{stem}. However, only two stem chambers were available.

472   Annual R_{stem} between the two were slightly different (264 $\pm$ 88 and 191 $\pm$ 64 g C m^{-2} yr^{-1})

473   highlighting the possible variation of R_{stem} for different trees. We did the measurement at a stem

474   height of 1.3 m. However, it has for some trees been found that stem CO_2 flux can vary with stem

475   height (Ceschia et al., 2002). This has been found to be caused by various amounts of CO_2

476 dissolved in the xylem that can diffuse out of the stem and therefore contribute to the apparent CO_2

477 flux measured by the chamber (Teskey and McGuire, 2002). Some of this CO_2 can be derived from

478 respiration produced elsewhere on the stem, or it can originate from CO_2 produced in the soil that is

479 being dissolved in the soil water, taken up by the roots and transported up through the stem (Aubrey

480 and Teskey, 2009; Bloemen et al., 2013; Teskey and Mcguire, 2007). Differences in R_{stem} along the

481 height of the stems could potentially have influenced the annual estimate of R_{stem}, as well as

482 differences in R_{stem} between different trees. This was, however, not tested in the current study.

483

484 **4.3 Different seasonal contribution of respiration components**

485 We found a strong seasonal pattern in the contributions of R_{soil} and R_{stem} to R_{eco} (Fig. 2). R_{eco}

486 generally followed the variation in temperature throughout the year with highest R_{eco} during the

487 summer growing season. This is usually seen for other temperate forest with growing season during

488 the warm and relatively wet summer (Janssens et al., 2000), in comparison to e.g. Mediterranean

489 ecosystems where R_{eco} is decoupled from temperature during the hot and dry summers, when water

490 becomes a limiting factor (Matteucci et al., 2015).

491 The variation in the different seasonal contributions of the individual components to R_{eco} have been

492 explained by differences in phenology, and their individual response to temperature (Migliavacca et

493 al., 2015). R_{stem} experienced dramatic differences in the contribution to R_{eco}, with 6 % during winter

494 and 16 % during summer. Although following an overall pattern similar to R_{soil} (Fig. 4), R_{stem} was

495 much lower during winter. The deciduous beech trees shed their leaves during autumn and enter a

496 dormant period until spring. During this period they do not photosynthesize, and transpiration is

497 limited to a minimum (Essiamah and Eschrich, 1986). Thus the transport through the xylem and

498 phloem is limited to a minimum and respiration is limited to only the necessary maintenance

499 respiration (Damesin, 2003). However, during the growing season growth respiration may be a

significant part of stem respiration, not directly determined by temperature, but by plant phenology (Lavigne and Ryan, 1997). The difference in R_{stem} throughout the year may therefore be larger than what can be expected from a general temperature dependence. Our observation of low R_{stem}, both in absolute terms and in its contribution to R_{eco} during the winter months, fits well with the pattern of tree dormancy during winter, and increased growth respiration during summer. Similar seasonal patterns of R_{stem} have been found in other temperate forests (Acosta et al., 2008; Edwards et al., 2002; Griffis et al., 2004; Shibistova et al., 2002; Yang et al., 2012, 2014). However, most studies do not measure R_{stem} during the winter months, making a full comparison difficult.

R_{soil} from the manual chambers differed dramatically from R_{stem} by showing a fairly similar contribution to R_{eco} during both winter, spring and summer of 52, 45 and 49 %, respectively, while the contribution increased to 79 % during autumn. Unlike the trees, the microorganisms in the soil do not go into dormancy and can continue to be active and respire, albeit at a slower rate, even during winter (Beverly and Franklin, 2015). Freezing temperatures, which causes the soil to freeze and lower R_{soil} dramatically can occur at our site. However, the winter period during this study was characterized by above-freezing temperatures during daytime for most of the winter; thereby leaving the entire soil column thawed at most times. The very high contribution of R_{soil} during autumn coincided with leaf senescence and litterfall. The input of litter to the soil is significant at the site, and has been found to account for 218 ± 17 g C m^{-2} yr^{-1} (Wu et al. 2013). Although the rate of R_{soil} is determined by temperature, the soil organisms will most often respond by increasing R_{soil} if additional organic matter such as litter is put into the soil (Han et al., 2015). A continuous high R_{soil} or a peak following litterfall has been found for other temperate forest ecosystems (DeForest et al., 2009; Hibbard et al., 2005). Thus, it is likely that the input of litter during autumn has kept R_{soil} at our site high by fuelling heterotrophic respiration. The trees, however, have shed their leaves and begun to enter dormancy, which lowers the relative contribution of plant respiration to R_{eco}.

The automated chamber measurements and the trenching revealed information on the contribution of autotrophic R_{soil} throughout the year. During summer, R_{soil} of the trenched soil plots was only 51 % of R_{soil} for the intact plots, while it increased to 83 % during autumn, which was comparable to the pre trenching level of 77 %. This indicated that autotrophic R_{soil} accounted for 49 % during summer. However, before the trenching in April, R_{soil} of the trenched plots was lower than the intact soil plots, by only accounted for 77 %, thus indicating heterogeneous undisturbed R_{soil}. Accounting for this pre trenching difference gives an autotrophic contribution of 34 % during summer.

The variation in the seasonal contribution of autotrophic R_{soil} with highest contribution during the plant growing season was expected and has been observed for several ecosystems (Beverly and Franklin, 2015; Pumpanen et al., 2015; Hanson et al., 2000). The major reason for the seasonal pattern of autotrophic R_{soil} is the seasonal pattern of GPP that drives an increase in root respiration during the growing season (Pumpanen et al., 2015). Hanson et al. (2000) reviewed the contribution of autotrophic R_{soil} for different ecosystems and found that the contribution of autotrophic respiration varied from 10 % to more than 90 %, with a mean value for forests of 45.8 %. 50 % autotrophic R_{soil} was found in a mixed beech spruce forest in the south of Germany (Andersen et al., 2005). Epron et al., (2001) found a mean autotrophic R_{soil} of 52 %, with highest autotrophic rate of 60 % in July in a French beech forest. Brumme (1995) found that autotrophic respiration comprised 40 % in a central German beech forest. Our trenching was performed in April, making a full comparison for the entire year impossible. Our estimate of an autotrophic contribution of 34 % during summer is relatively low compared to prior literature values. However, since the trenching was only performed a few months prior to the measurements, it is possible that decomposing root litter from the severed roots may have contributed to the trenched plots, thereby leading to an overestimated heterotrophic R_{soil} (Díaz-Pinés et al., 2010; Epron et al., 1999; Hanson et al., 2000;

547 Silver et al., 2005; Subke et al., 2006). A second possibility is the presence of deeper living roots

548 below the trenching depth of 25 cm.

549 Instead of following the variation in GPP, R_{stem} more closely followed R_{soil} and temperature during

550 spring, summer and autumn (Fig. 4, Fig. 3). Thus the high variation in GPP during the growing

551 season was not seen for R_{stem}, which could indicate that the magnitude of R_{stem} was independent

552 from the day to day variations in GPP and the associated high respiration rates that are expected for

553 the photosynthesizing organs. The dependence on temperature is in line with other studies that have

554 found a clear temperature dependence of R_{stem} (Harris et al., 2008; Lavigne et al., 1996; Ryan et al.,

555 1995), although photosynthesis has also been found to partially regulate stem respiration (Zha et al.,

556 2004).

557

558 **4.4 Diel patterns of respiration**

559 Both R_{stem} and R_{root} showed a clear diel pattern during summer with the highest respiration seen

560 around 13:00-15:00 CET for R_{stem}, and the highest respiration seen from 9:00-15:00 for R_{root} (Fig.

561 5o, k). The high R_{stem} during the afternoon is consistent with the findings of other studies (Acosta et

562 al., 2008; Teskey and Mcguire, 2007; Zha et al., 2004). This distinct diel pattern have been

563 explained by a temperature response to the diel pattern of temperature (Teskey and Mcguire, 2007).

564 However, other studies have found diel patterns of R_{stem} different from the diel pattern of

565 temperature, which has been suggested to be due to the diel pattern of R_{stem} being modified by

566 photosynthesis and cambium activity independent of temperature (Yang et al., 2014). The diel

567 pattern of R_{stem} during summer in our study followed the diel pattern of air temperature, thus

568 suggesting that temperature is a main determining factor for R_{stem} at our site. This is in line with

569 temperature being the determining factor for R_{stem} at the seasonal scale (Fig. 4, Section 4.3).

570 However, during winter R_{stem} was very low and showed no diel pattern, which could reflect the tree

571 dormancy during this period (Fig. 5m). The high R_{root} during 9:00-15:00 is consistent with the

572 findings of other studies that saw highest R_{root} during daytime, which often has been found to be

573 linked with photosynthesis (Chen et al., 2010; Drake et al., 2008; Lai et al., 2016; Wertin and

574 Teskey, 2008). During daytime, an increase in R_{root} is seen due to respiration of recently fixed

575 photosynthates. During nighttime, however, no photosynthesis takes place, leading to the diel

576 pattern in feeding of photosynthates. Photosynthesis at the DK-Sor site usually peaks at noon,

577 before the peak in temperature (Pilegaard et al., 2001). This is consistent with the peak in R_{root} in

578 this study, thus indicating that photosynthates might in part determine the diel pattern of R_{root} during

579 summer. Interestingly, no diel pattern was seen during winter and autumn (Fig. 5i, l). During

580 winter, no photosynthesis takes place, and only little photosynthesis takes place in autumn, thus

581 only a small amount of photosynthates can alter the diel pattern during these periods. During spring,

582 however, a small peak was seen around 15:00 CET, later than the peak seen during summer (Fig.

583 5j). Spring was the only season that showed a diel pattern of soil temperature at 5 cm depth (Fig.

584 6b). Thus, it is possible that the temperature response of R_{root} is dominant during spring.

585 No clear difference in the diel pattern of R_{soil} was seen between the intact and trenched soil plots

586 (Fig. 5a-h). However, the trenched plots had lower R_{soil} following the trenching, indicating that the

587 autotrophic contribution to R_{soil} had been completely or partly removed from the trenched plots

588 (Section 4.3). Heterotrophic R_{soil} has generally been found to respond to temperature on a seasonal

589 scale, as well as on a diel scale, although a hysteresis on the diel scale between soil temperature and

590 heterotrophic R_{soil} has also been observed (Chen et al., 2009; Song et al., 2015; Zhang et al., 2015).

591 In contrast, autotrophic R_{soil} has often been found to be decoupled from temperature on a diel scale,

592 resulting primarily from substrate transfer to the soil bacteria through carbon exudates from plant

593 roots (Kuzyakov and Gavrichkova, 2010). Similarly to the increase in R_{root} as a result of increased

594 levels of fresh photosynthates, the increase in R_{soil} has been found to lag after photosynthesis

595 (Savage et al., 2013; Tang et al., 2005). Whereas we saw an increase in R_{root} during daytime, we did

596 not see a similar increase in R_{soil} during daytime in the intact soil plot that contained roots. Instead,

597 a lower daytime R_{soil} was seen for both the intact and trenched soil plots. Soil temperature at 5 cm

598 depth generally showed no diel pattern for winter, summer and autumn, which would mean no diel

599 pattern in R_{soil} if only determined by temperature (Fig. 6). It was surprising that no difference was

600 seen between the intact and trenched soil plots. In a previous study at the site, the diel pattern of

601 R_{soil} was investigated for intact soil (Brændholt et al. 2017). A similar diel pattern with lower

602 daytime R_{soil} was observed. However, it was found that the measured soil CO_2 fluxes were

603 influenced by low atmospheric turbulence, which was found to lead to an overestimation of

604 measured soil CO_2 fluxes especially during nighttime, which in turn also biased the diel pattern. In

605 the current study, we removed measurements at low atmospheric turbulence to remove the effect of

606 overestimation of fluxes, as recommended by Brændholt et al. (2017). It is, however, possible that

607 overestimation still plays a role. If this effect is larger than the potential differences in the diel

608 patterns of intact soil and trenched soil, then this effect may overrule the real diel patterns, making

609 it difficult to make a distinction between the diel patterns.

610

611 5 Conclusions

612 In this study we used the eddy covariance technique together with manual and automated closed-

613 chambers to quantify the individual components of ecosystem respiration at diel, seasonal and

614 annual scale. We found that the contribution of R_{stem} to total R_{eco} varied throughout the year, by only

615 accounting for 6 % of R_{eco} during winter and 16 % during the summer growing season. In contrast,

616 R_{soil} showed a fairly similar contribution to R_{eco} during winter, spring and summer of 52, 45 and 49

617 %, respectively, while the contribution increased to 79 % during autumn. We attributed the large

618 difference in the seasonal contribution of R_{stem} to different phenological stages of dormancy and

619 growth experienced for the trees during the year, whereas we attributed the high contribution of R_{soil}

620 in autumn to the large input of litter from the deciduous beech trees.

621 By the trenching method, we partitioned R_{soil} into its heterotrophic and autotrophic components. We

622 found that autotrophic R_{soil} accounted for 34 % of R_{soil} during summer, a relative low value

623 compared to findings from other studies. However, we could not rule out the possibility that

624 decomposing roots from the trenched soil plots might have led to an overestimated heterotrophic

625 R_{soil}.

626 Diel R_{stem} and R_{root} showed a clear pattern during summer with the highest respiration seen around

627 13:00-15:00 CET for R_{stem}, and the highest respiration seen from 9:00-15:00 for R_{root}. In contrast,

628 R_{soil} showed the lowest respiration during daytime R_{soil} with no clear difference in the diel pattern

629 between the intact and trenched soil plots.

630 Finally, we calculated annual R_{soil} for different transects at the site, and found that annual R_{soil}

631 estimated from the previously used transect at the site was underestimated due to R_{soil} of the transect

632 not being representative for the spatial heterogeneity of R_{soil} at the site. This highlighted the

633 importance of performing a sufficient number of manual chamber measurements at a site to

634 adequately capture the spatial variation in R_{soil}, and thereby to correctly estimate R_{soil}.

635

Acknowledgements

639

References

Acosta, M., Pavelka, M., Pokorný, R., Janouš, D., Marek, M.V., 2008. Seasonal variation in CO_2 efflux of stems and branches of Norway spruce trees. Ann. Bot. 101, 469–477.

Andersen, C.P., Nikolov, I., Nikolova, P., Matyssek, R., Häberle, K.H., 2005. Estimating "autotrophic" belowground respiration in spruce and beech forests: Decreases following girdling. Eur. J. For. Res. 124, 155–163.

Aubrey, D.P., Teskey, R.O., 2009. Root-derived CO_2 efflux via xylem stream rivals soil CO_2 efflux. New Phytol. 184, 35–40.

Baggs, E.M., 2006. Partitioning the components of soil respiration: A research challenge. Plant Soil. 284, 1–5.

Beer, C., Reichstein, M., Tomelleri, E., Ciais, P., Jung, M., Carvalhais, N., Rödenbeck, C., Arain, M.A., Baldocchi, D., Bonan, G.B., Bondeau, A., Cescatti, A., Lasslop, G., Lindroth, A., Lomas, M., Luyssaert, S., Margolis, H., Oleson, K.W., Roupsard, O., Veenendaal, E., Viovy, N., Williams, C., Woodward, F.I., Papale, D., 2010. Terrestrial gross carbon dioxide uptake: Global distribution and covariation with climate. Science. 329, 834-838.

Beverly, D., Franklin, S., 2015. Heterotrophic and Autotrophic Soil Respiration under Simulated Dormancy Conditions. Open J. For. 5, 274–286.

Bloemen, J., Mcguire, M.A., Aubrey, D.P., Teskey, R.O., Steppe, K., 2013. Transport of root-respired CO_2 via the transpiration stream affects aboveground carbon assimilation and CO_2 efflux in trees. New Phytol. 197, 555–565.

Bond-Lamberty, B., Bronson, D., Bladyka, E., Gower, S.T., 2011. A comparison of trenched plot techniques for partitioning soil respiration. Soil Biol. Biochem. 43, 2108–2114.

Brændholt, A., Larsen, K.S., Ibrom, A., Pilegaard, K., 2017. Overestimation of closed-chamber soil CO_2 effluxes at low atmospheric turbulence. Biogeosciences. 14, 1603-1616.

664 Brumme, R., 1995. Mechanisms of carbon and nutrient release and retention in beech forest gaps.

665   Plant Soil. 168-169, 593–600.

666 Ceschia, É., Damesin, C., Lebaube, S., Pontailler, J.Y., Dufrêne, É., 2002. Spatial and seasonal

667   variations in stem respiration of beech trees (*Fagus sylvatica*). Ann. For. Sci. 59, 801–812.

668 Chen, D., Zhou, L., Rao, X., Lin, Y., Fu, S., 2010. Effects of root diameter and root nitrogen

669   concentration on in situ root respiration among different seasons and tree species. Ecol. Res.

670   25, 983–993.

671 Chen, J.M., Huang, S.E., Ju, W., Gaumont-Guay, D., Black, T.A., 2009. Daily heterotrophic

672   respiration model considering the diurnal temperature variability in the soil. J. Geophys. Res.

673   114, G01022, 1-11.

674 Ciais, P., Reichstein, M., Viovy, N., Granier, A., Ogée, J., Allard, V., Aubinet, M., Buchmann, N.,

675   Bernhofer, C., Carrara, A., Chevallier, F., De Noblet, N., Friend, A.D., Friedlingstein, P.,

676   Grünwald, T., Heinesch, B., Keronen, P., Knohl, A., Krinner, G., Loustau, D., Manca, G.,

677   Matteucci, G., Miglietta, F., Ourcival, J.M., Papale, D., Pilegaard, K., Rambal, S., Seufert, G.,

678   Soussana, J.F., Sanz, M.J., Schulze, E.D., Vesala, T., Valentini, R., 2005. Europe-wide

679   reduction in primary productivity caused by the heat and drought in 2003. Nature. 437, 529–

680   533.

681 Damesin, C., 2003. Respiration and photosynthesis characteristics of current-year stems of Fagus

682   sylvatica: From the seasonal pattern to an annual balance. New Phytol. 158, 465–475.

683 Damesin, C., Ceschia, E., Le Goff, N., Ottorini, J.M., Dufrene, E. 2002. Stem and branch

684   respiration of beech: from tree measurements to estimations at the stand level. New Phytol.

685   153, 159–172.

686 Davidson, E.A., Savage, K., Verchot, L.V., Navarro, R., 2002. Minimizing artifacts and biases in

687   chamber-based measurements of soil respiration. Agric. For. Meteorol. 113, 21–37.

688 DeForest, J.L., Chen, J., McNulty, S.G., 2009. Leaf litter is an important mediator of soil respiration

689   in an oak-dominated forest. Int. J. Biometeorol. 53, 127–134.

690 Department of Biogeochemical Integration, MPI Jena, 2017. REddyProc: Eddy covariance data

691   processing tool. http://www.bgc-jena.mpg.de/REddyProc/brew/REddyProc.rhtml (accessed

692   17.05.29).

693 Díaz-Pinés, E., Schindlbacher, A., Pfever, M., Jandl, R., Zechmeister-Boltenstern, S., Rubio, A.,

694   2010. Root trenching: A useful tool to estimate autotrophic soil respiration? A case study in an

695   austrian mountain forest. Eur. J. For. Res. 129, 101–109.

696 Drake, J.E., Stoy, P.C., Jackson, R.B., DeLucia, E.H., 2008. Fine-root respiration in a loblolly pine

697   (*Pinus taeda* L.) forest exposed to elevated CO_2 and N fertilization. Plant, Cell Environ. 31,

698   1663–1672.

699 Edwards, N.T., Hanson, P.J., 1996. Stem respiration in a closed-canopy upland oak forest. Tree

700   Physiol. 16, 433–439.

701 Edwards, N.T., Tschaplinski, T.J., Norby, R.J., 2002. Stem respiration increases in CO_2-enriched

702   sweetgum trees. New Phytol. 155, 239–248.

703 Elzhov, V.T., Mullen, K.M., Spiess, A., Bolker, B., 2016. minpack.lm: R Interface to the

704   Levenberg-Marquardt Nonlinear Least-Squares Algorithm Found in MINPACK, Plus Support

705   for Bounds, R package version 1.2-0. http://CRAN.R-project.org/package=minpack.lm

706   (accessed 17.05.29).

707 Epron, D., Farque, L., Lucot, E., Badot, P.M., 1999. Efflux in a Beech Forest: the Contribution of

708   Root Respiration. Ann. For. Sci. 56, 289–295.

709 Epron, D., Le Dantec, V., Dufrene, E., Granier, A., 2001. Seasonal dynamics of soil carbon dioxide

710   efflux and simulated rhizosphere respiration in a beech forest. Tree Physiol. 21, 145–152.

31

711   Essiamah, S., Eschrich, W., 1986. Water Uptake in Deciduous Trees During Winter and the Role of

712   Conducting Tissues in Spring Reactivation. IAWA Journal. 7, 31-38.

713   Griffis, T.J., Black, T.A., Gaumont-Guay, D., Drewitt, G.B., Nesic, Z., Barr, A.G., Morgenstern,

714   K., Kljun, N., 2004. Seasonal variation and partitioning of ecosystem respiration in a southern

715   boreal aspen forest. Agric. For. Meteorol. 125, 207–223.

716   Hanson, P.J., Edwards, N.T., Garten, C.T., Andrews, J.A., 2000. Separating root and soil microbial

717   contributions to soil respiration: A review of methods and observations. Biogeochemistry. 48,

718   115–146.

719   Han, T., Huang, W., Liu, J., Zhou, G., Xiao, Y., 2015. Different soil respiration responses to litter

720   manipulation in three subtropical successional forests. Sci. Rep. 5, 18166.

721   Harris, N.L., Hall, C.A.S., Lugo, A.E., 2008. Estimates of species- and ecosystem-level respiration

722   of woody stems along an elevational gradient in the Luquillo Mountains, Puerto Rico. Ecol.

723   Modell. 216, 253–264.

724   Hibbard, K.A., Law, B.E., Reichstein, M., Sulzman, J., 2005. An analysis of soil respiration across

725   northern hemisphere temperate ecosystems. Biogeochemistry. 73, 29–70.

726   Högberg, P., Nordgren, A., Högberg, M.N., Ottosson-Lofvenius, M., Bhupinderpal, S., Olsson, P.,

727   Linder, S., 2005. Fractional contributions by autotrophic and heterotrophic respiration to soil-

728   surface CO_2 efflux in boreal forests. SEB Exp Biol Ser. 251–267.

729   Hutchinson, G.L., Mosier, A.R., 1981. Improved soil cover method for field measurement of

730   nitrous oxide fluxes. Soil Sci. Soc. Am. J. 45, 311–316.

731   Ibrom, A., Jarvis, P.G., Clement, R.B., Morgenstern, K., Oltchev, A., Medlyn, B., Wang, Y.P.,

732   Wingate, L., Moncrieff, J., Gravenhorst, G., 2006. A comparative analysis of simulated and

733   observed photosynthetic CO_2 uptake in two coniferous forest canopies. Tree Physiol. 26, 845–

734   864.

735   Inoue, A., 2004. Relationships of stem surface area to other stem dimensions for Japanese cedar

736   (*Cryptomeria japonica* D. Don) and Japanese cypress (*Chamaecyparis obtusa* Endl.) trees. J.

737   For. Res. 9, 45–50.

738   IPCC, 2013. Climate Change 2013: the Physical Science Basis. Contribution of Working Group I to

739   the Fifth Assessment Report of the Intergovernmental Panel on Climate Change. Cambridge

740   University Press, Cambridge, United Kingdom and New York, NY, USA. 1535.

741   Janssens, I., Pilegard, K., 2003. Large seasonal changes in Q_{10} of soil respiration in a beech forest.

742   Global Biogeochem. Cycles. 9, 911–918.

743   Janssens, I.A., Lankreijer, H., Matteucci, G., Kowalski, A.S., Buchmann, N., Epron, D., Pilegaard,

744   K., Kutsch, W., Longdoz, B., Grünwald, T., Montagnani, L., Dore, S., Rebmann, C., Moors, E.

745   J., Grelle, A., Rannik, Ü., Morgenstern, K., Oltchev, S., Clement, R., Gudmundsson, J.,

746   Minerbi, S., Berbigier, P., Ibrom, A., Moncrieff, J., Aubinet, M., Bernhofer, C., Jensen, N.O.,

747   Vesala, T., Granier, A., Schulze, E.D., Lindroth, A., Dolman, A.J., Jarvis, P.G., Ceulemans, R.,

748   Valentini, R., 2000. Productivity overshadows temperature in determining soil and ecosystem

749   respiration across European forests. Glob. Chang. Biol. 7, 269–278.

750   Knohl, A., Søe, A.R.B., Kutsch, W.L., Göckede, M., Buchmann, N., 2008. Representative estimates

751   of soil and ecosystem respiration in an old beech forest. Plant Soil. 302, 189–202.

752   Kuzyakov, Y., Gavrichkova, O., 2010. Time lag between photosynthesis and carbon dioxide efflux

753   from soil: A review of mechanisms and controls. Glob. Chang. Biol. 16, 3386–3406.

754   Lai, Z., Lu, S., Zhang, Y., Wu, B., Qin, S., Feng, W., Liu, J., Fa, K., 2016. Diel patterns of fine root

755   respiration in a dryland shrub, measured in situ over different phenological stages. J. For. Res.

756   21, 31–42.

757   Landesverwaltungsamt Sachsen-Anhalt, 2011. Leitfaden zur Vorratsermittlung von Waldbeständen

758   und zur Bewertung forstrechtlicher Sachverhalte (In german). https://lvwa.sachsen-

759 anhalt.de/fileadmin/Bibliothek/Politik_und_Verwaltung/LVWA/LVwA/Dokumente/pressestell

760 e/publikationen/broschueren/vorratsermittlung.pdf (accessed 17.05.29).

761 Lasslop, G., Reichstein, M., Papale, D., Richardson, A., Arneth, A., Barr, A., Stoy, P., Wohlfahrt,

762 G., 2010. Separation of net ecosystem exchange into assimilation and respiration using a light

763 response curve approach: critical issues and global evaluation. Glob. Chang. Biol. 16, 187-208.

764 Lavigne, M.B., Franklin, S.E., Hunt Jr, E.R., 1996. Estimating stem maintenance respiration rates

765 of dissimilar balsam fir stands. Tree Physiol. 16, 687–95.

766 Lavigne, M.B., Ryan, M.G., 1997. Growth and maintenance respiration rates of aspen, black spruce

767 and jack pine stems at northern and southern BOREAS sites. Tree Physiol. 17, 543–551.

768 Lloyd, J., Taylor, J.A., 1994. On the temperature dependence of soil respiration. Funct. Ecol. 8,

769 315–323.

770 Luyssaert, S., Inglima, I., Jung, M., Richardson, A.D., Reichstein, M., Papale, D., Piao, S.L.,

771 Schulze, E.D., Wingate, L., Matteucci, G., Aragao, L., Aubinet, M., Beer, C., Bernhofer, C.,

772 Black, K.G., Bonal, D., Bonnefond, J.M., Chambers, J., Ciais, P., Cook, B., Davis, K.J.,

773 Dolman, A.J., Gielen, B., Goulden, M., Grace, J., Granier, A., Grelle, A., Griffis, T.,

774 Grünwald, T., Guidolotti, G., Hanson, P.J., Harding, R., Hollinger, D.Y., Hutyra, L.R., Kolari,

775 P., Kruijt, B., Kutsch, W., Lagergren, F., Laurila, T., Law, B.E., Le Maire, G., Lindroth, A.,

776 Loustau, D., Malhi, Y., Mateus, J., Migliavacca, M., Misson, L., Montagnani, L., Moncrieff,

777 J., Moors, E., Munger, J.W., Nikinmaa, E., Ollinger, S.V., Pita, G., Rebmann, C., Roupsard,

778 O., Saigusa, N., Sanz, M.J., Seufert, G., Sierra, C., Smith, M.L., Tang, J., Valentini, R., Vesala,

779 T., Janssens, I.A., 2007. CO_2 balance of boreal, temperate, and tropical forests derived from a

780 global database. Glob. Chang. Biol. 13, 2509–2537.

781 Mahecha, M.D., Reichstein, M., Carvalhais, N., Lasslop, G., Lange, H., Seneviratne, S.I., Vargas,

782 R., Ammann, C., Arain, M.A., Cescatti, A., Janssens, I.A., Migliavacca, M., Montagnani, L.,

783   Richardson, A.D., 2010. Global Convergence in the Temperature Sensitivity of Respiration at

784   Ecosystem Level, Science. 329, 838–840.

785   Matteucci, M., Gruening, C., Goded Ballarin, I., Seufert, G., Cescatti, A., 2015. Components,

786   drivers and temporal dynamics of ecosystem respiration in a Mediterranean pine forest. Soil

787   Biol. Biochem. 88, 224–235.

788   Migliavacca, M., Reichstein, M., Richardson, A.D., Mahecha, M.D., Cremonese, E., Delpierre, N.,

789   Galvagno, M., Law, B.E., Wohlfahrt, G., Andrew Black, T., Carvalhais, N., Ceccherini, G.,

790   Chen, J., Gobron, N., Koffi, E., William Munger, J., Perez-Priego, O., Robustelli, M.,

791   Tomelleri, E., Cescatti, A., 2015. Influence of physiological phenology on the seasonal pattern

792   of ecosystem respiration in deciduous forests. Glob. Chang. Biol. 21, 363–376.

793   Nagy, M.T., Janssens, I.A., Curiel Yuste, J., Carrara, A., Ceulemans, R., 2006. Footprint-adjusted

794   net ecosystem CO_2 exchange and carbon balance components of a temperate forest. Agric. For.

795   Meteorol. 139, 344–360.

796   Østergård, J., 2000. Jordbundsdannelse under bøgeskov og mark ved Lille Bøgeskov, Sorø.

797   Master's thesis, Department of Earth Sciences, University of Aarhus, Denmark, (in Danish).

798   Peichl, M., Sonnentag, O., Wohlfahrt G., Flanagan, L.B., Baldocchi, D.D., Kiely, G., Galvagno, M.,

799   Gianelle, D., Marcolla, B., Pio, C., Migliavacca, M., Jones, M.B., Saunders, M., 2013.

800   Convergence of potential net ecosystem production among contrasting C_3 grasslands. Ecology

801   Letters. 16, 502–512.

802   Pilegaard, K., Hummelshøj, P., Jensen, N.O., Chen, Z., 2001. Two years of continuous CO_2 eddy-

803   flux measurements over a Danish beech forest. 107, 29–41.

804   Pilegaard, K., Ibrom, A., Courtney, M.S., Hummelshøj, P., Jensen, N.O., 2011. Increasing net CO_2

805   uptake by a Danish beech forest during the period from 1996 to 2009. Agric. For. Meteorol.

806   151, 934–946.

807   Pumpanen, J., Kulmala, L., Lindén, A., Kolari, P., Nikinmaa, E., 2015. Seasonal dynamics of

808   autotrophic respiration in boreal forest soil estimated by continuous chamber measurements.

809   Boreal Environ. Res. 20, 637–650.

810   R Core Team, 2014. R: A language and environment for statistical computing. R Foundation for

811   Statistical Computing, Vienna, Austria.

812   Reichstein, M., Falge, E., Baldocchi, D., Papale, D., Aubinet, M., Berbigier, P., Bernhofer, C.,

813   Buchmann, N., Gilmanov, T., Granier, A., Grünwald, T., Havránková, K., Ilvesniemi, H.,

814   Janous, D., Knohl, A., Laurila, T., Lohila, A., Loustau, D., Matteucci, G., Meyers, T.,

815   Miglietta, F., Ourcival, J.M., Pumpanen, J., Rambal, S., Rotenberg, E., Sanz, M., Tenhunen, J.,

816   Seufert, G., Vaccari, F., Vesala, T., Yakir, D., Valentini, R., 2005. On the separation of net

817   ecosystem exchange into assimilation and ecosystem respiration: Review and improved

818   algorithm. Glob. Chang. Biol. 11, 1424–1439.

819   Rodeghiero, M., Cescatti, A., 2006. Indirect partitioning of soil respiration in a series of evergreen

820   forest ecosystems. Plant Soil. 284, 7–22.

821   Rodríguez-Calcerrada, J., Martin-StPaul, N.K., Lempereur, M., Ourcival, J.M., Rey, M. del C. del,

822   Joffre, R., Rambal, S., 2014. Stem CO_2 efflux and its contribution to ecosystem CO_2 efflux

823   decrease with drought in a Mediterranean forest stand. Agric. For. Meteorol. 195–196, 61–72.

824   Ryan, M.G., Gower, S.T., Hubbard, R.M., Waring, R.H., Gholz, H.L., Cropper, W.P., Running,

825   S.W., 1995. Woody tissue maintenance respiration of four conifers in contrasting climates.

826   Oecologia. 101, 133–140.

827   Savage, K., Davidson, E.A., Richardson, D.A., 2008. A conceptual and practical approach to data

828   quality and analysis procedures for high-frequency soil respiration measurements. Funct. Ecol.

829   22, 1000–1007.

830 Savage, K., Davidson, E.A., Tang, J., 2013. Diel patterns of autotrophic and heterotrophic

831   respiration among phenological stages. Glob. Chang. Biol. 19, 1151–1159.

832 Savage, K.E., Davidson, E.A., 2003. A comparison of manual and automated systems for soil CO_2

833   flux measurements: Trade-offs between spatial and temporal resolution. J. Exp. Bot. 54, 891–

834   899.

835 Saveyn, A., Steppe, K., Lemeur, R., 2007. Daytime depression in tree stem CO_2 efflux rates: Is it

836   caused by low stem turgor pressure? Ann. Bot. 99, 477–485.

837 Schimel, D.S., House, J.I., Hibbard, K.A, Bousquet, P., Ciais, P., Peylin, P., Braswell, B.H., Apps,

838   M.J., Baker, D., Bondeau, A, Canadell, J., Churkina, G., Cramer, W., Denning, A.S., Field,

839   C.B., Friedlingstein, P., Goodale, C., Heimann, M., Houghton, R.A., Melillo, J.M., Moore, B.,

840   Murdiyarso, D., Noble, I., Pacala, S.W., Prentice, I.C., Raupach, M.R., Rayner, P.J., Scholes,

841   R.J., Steffen, W.L., Wirth, C., 2001. Recent patterns and mechanisms of carbon exchange by

842   terrestrial ecosystems. Nature. 414, 169–172.

843 Shibistova, O., Lloyd, J., Zrazhevskaya, G., Arneth, A., Kolle, O., Knohl, A., Astrakhantceva, N.,

844   Shijneva, I., Schmerler, J., 2002. Annual ecosystem respiration budget for a *Pinus sylvestris*

845   stand in central Siberia. Tellus. 54B, 568–589.

846 Silver, W.L., Thompson, A.W., McGroddy, M.E., Varner, R.K., Dias, J.D., Silva, H., Crill, P.M.,

847   Keller, M., 2005. Fine root dynamics and trace gas fluxes in two lowland tropical forest soils.

848   Glob. Chang. Biol. 11, 290–306.

849 Song, W., Chen, S., Zhou, Y., Wu, B., Zhu, Y., Lu, Q., Lin, G., 2015. Contrasting diel hysteresis

850   between soil autotrophic and heterotrophic respiration in a desert ecosystem under different

851   rainfall scenarios. Sci Rep. 5, 16779.

852 Subke, J.A., Inglima, I., Cotrufo, M.F., 2006. Trends and methodological impacts in soil CO_2 efflux

853   partitioning: A metaanalytical review. Glob. Chang. Biol. 12, 921–943.

854   Tang, J., Baldocchi, D.D., Xu, L., 2005. Tree photosynthesis modulates soil respiration on a diurnal

855   time scale. Glob. Chang. Biol. 11, 1298–1304.

856   Tang, J., Bolstad, P.V., Desai, A.R., Martin, J.G., Cook, B.D., Davis, K.J., Carey, E.V., 2008.

857   Ecosystem respiration and its components in an old-growth forest in the Great Lakes region of

858   the United States. Agric. For. Meteorol. 148, 171–185.

859   Teskey, R.O., McGuire, M.A., 2002. Carbon dioxide transport in xylem causes errors in estimation

860   of rates of respiration in stems and branches of trees. Plant, Cell Environ. 25, 1571–1577.

861   Teskey, R.O., Mcguire, M.A., 2007. Measurement of stem respiration of sycamore (*Platanus*

862   *occidentalis* L.) trees involves internal and external fluxes of CO_2 and possible transport of

863   CO_2 from roots. Plant, Cell Environ. 30, 570–579.

864   Valentini, R., Matteucci, G., Dolman, A.J., Schulze, E.D., Jarvis, P.G., 2003. The carbon sink

865   strength of forests in Europe: a synthesis of results. In: Valentini, R. (Ed.), Fluxes of Carbon,

866   Water and Energy of European Forests, Ecological Studies, vol. 163. Springer, Berlin.

867   Van Oijen, M., Rougier, J., Smith, R., 2005. Bayesian calibration of process-based forest models:

868   bridging the gap between models and data. Tree Physiol. 25 (7), 915–927.

869   Wang, M., Guan, D.X., Han, S.J., Wu, J.L., 2010. Comparison of eddy covariance and chamber-

870   based methods for measuring CO_2 flux in a temperate mixed forest. Tree Physiol. 30, 149–163.

871   Webster, K.L., Creed, I.F., Bourbonnière, R.A., Beall, F.D., 2008. Controls on the heterogeneity of

872   soil respiration in a tolerant hardwood forest. J. Geophys. Res. Biogeosciences 113, 1–15.

873   Wertin, T.M., Teskey, R.O., 2008. Close coupling of whole-plant respiration to net photosynthesis

874   and carbohydrates. Tree Physiol. 28, 1831–40.

875   Wofsy, S.C., Goulden, M.L., Munger, J.W., Fan, S.M., Bakwin, P.S., Daube, B.C., Bassow, S.L.,

876   Bazzaz, F.A., 1993. Net exchange of CO_2 in a mid-latitude forest. Science. 260, 1314 – 1317.

877 Wu, J., Larsen, K.S., van der Linden, L., Beier, C., Pilegaard, K., Ibrom, A., 2013. Synthesis on the
878   carbon budget and cycling in a Danish, temperate deciduous forest. Agric. For. Meteorol. 181,
879   94–107.

880 Yang, J., He, Y., Aubrey, D.P., Zhuang, Q., Teskey, R.O., 2015. Global patterns and predictors of
881   stem CO_2 efflux in forest ecosystems. Glob. Chang. Biol. 22, 1433–1444.

882 Yang, J.Y., Teskey, R.O., Wang, C.K., 2012. Stem CO_2 efflux of ten species in temperate forests in
883   Northeastern China. Trees - Struct. Funct. 26, 1225–1235.

884 Yang, Y., Zhao, M., Xu, X., Sun, Z., Yin, G., Piao, S., 2014. Diurnal and seasonal change in stem
885   respiration of Larix principis-rupprechtii trees, northern China. PLoS One. 9, 1–7.

886 Zha, T., Kellomäki, S., Wang, K.Y., Ryyppö, A., Niinistö, S., 2004. Seasonal and annual stem
887   respiration of scots pine trees under boreal conditions. Ann. Bot. 94, 889–896.

888 Zhang, Q., Katul, G.G., Oren, R., Daly, E., Manzoni, S., Yang, D., Al, Z.E.T., 2015. The hysteresis
889   response of soil CO_2 concentration and soil respiration to soil temperature. J. Geophys. Res.
890   Biogeosci. 120, 1605–1618.

891 Zhu, L.W., Zhao, P., Ni, G.Y., Cao, Q.P., Zhou, C.M., Zeng, X.P., 2012. Individual-and stand-level
892   stem CO_2 efflux in a subtropical *Schima superba* plantation. Biogeosciences. 9, 3729–3737.

893

894
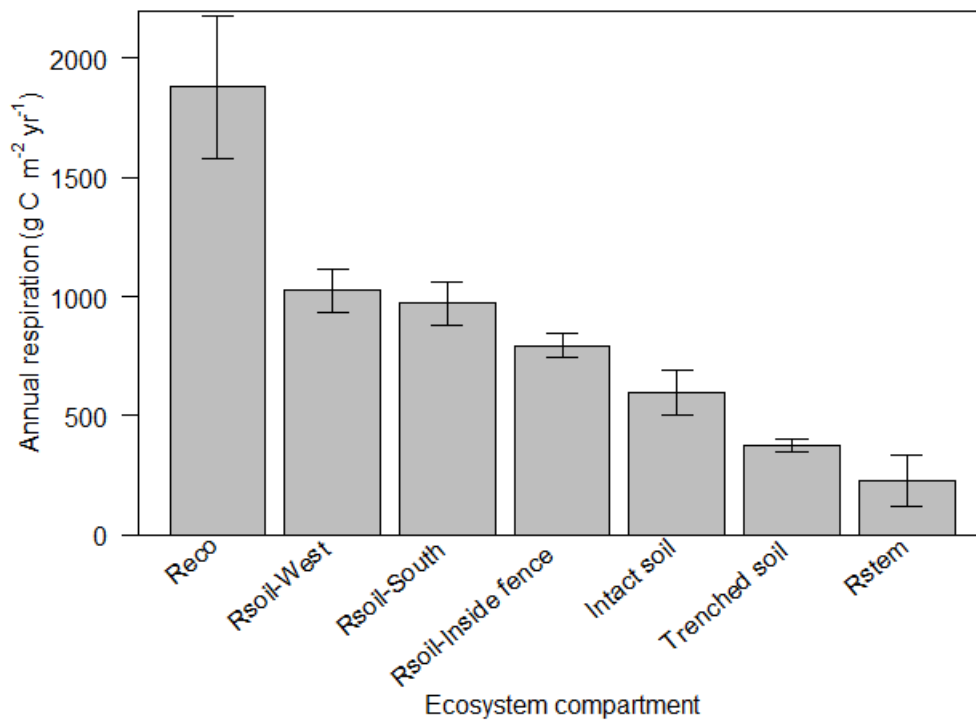
Figure 1: Annual respiration for the different components of the ecosystem, with the estimated uncertainties shown by error bars. From left to right the bars show: R_{eco}, R_{soil} at the west transect, R_{soil} at the south transect, R_{soil} at the inside fence transect, R_{soil} at the intact soil plots measured by the automated chambers, R_{soil} at the trenched soil plots measured by the automated chambers and R_{stem}. The annual estimated GPP was 2272 ± 136 g C m^{-2} yr^{-1}.

900

901
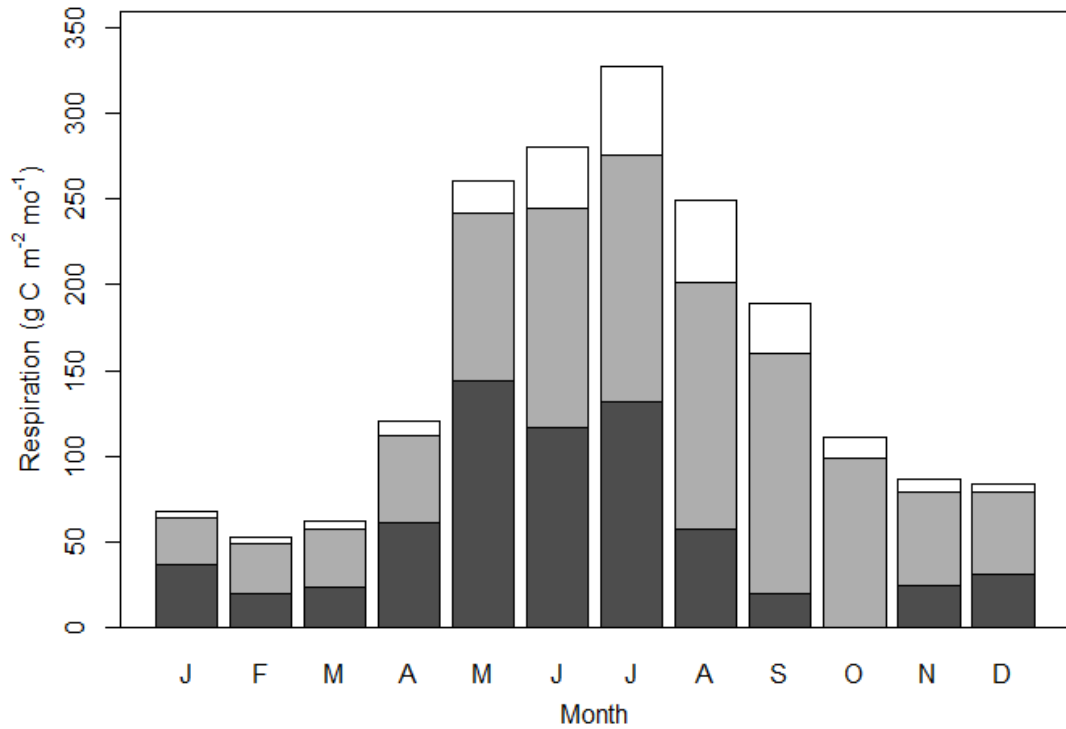
Figure 2: R_{eco} (total bar height) partitioned into the component respiration rates from R_{soil} (grey)

and R_{stem} (white) on a surface area basis for each month of 2016. The black bars represent the

remaining R_{eco} after R_{soil} and R_{stem} have been subtracted, i.e. from tree branches and leaves. For the

monthly R_{soil}, the average of the manual closed-chamber measurements of the south and west

transect is shown. Note, that for October, R_{eco} was 11.9 g C m^{-2} yr^{-1} lower than the sum of R_{stem} and
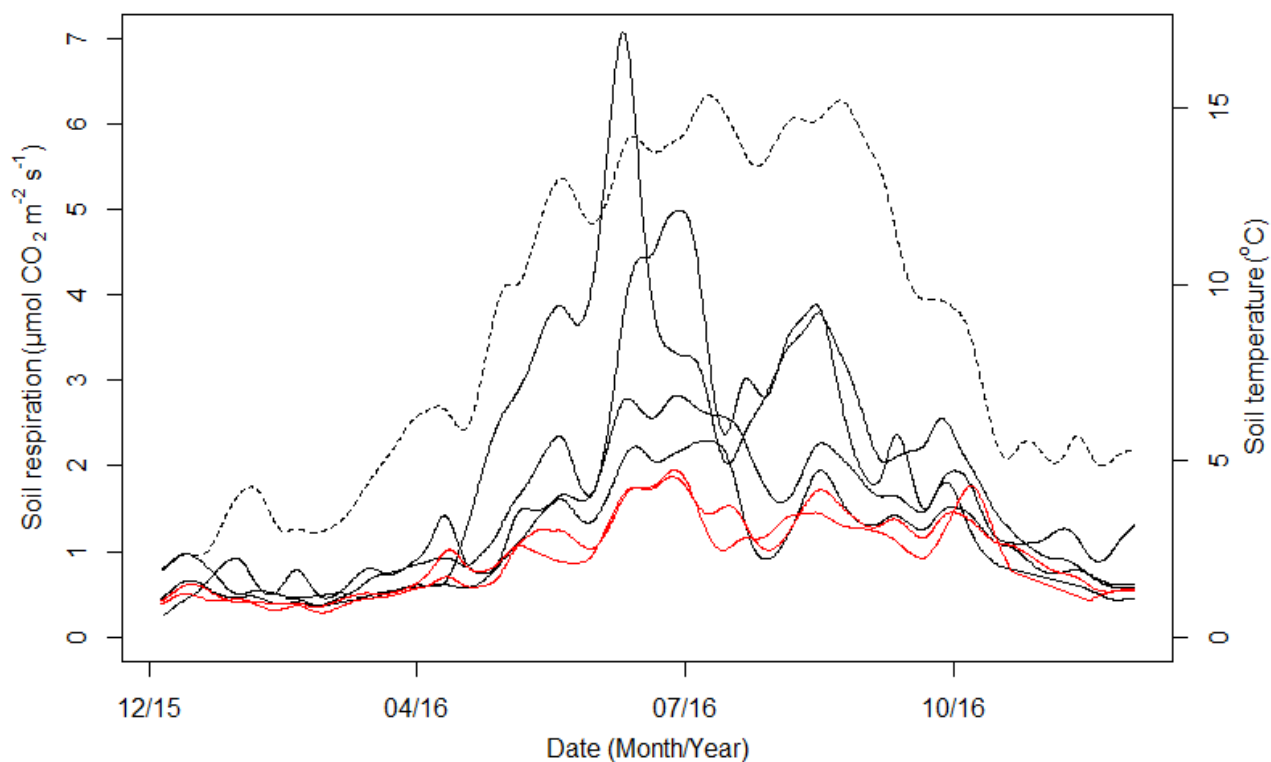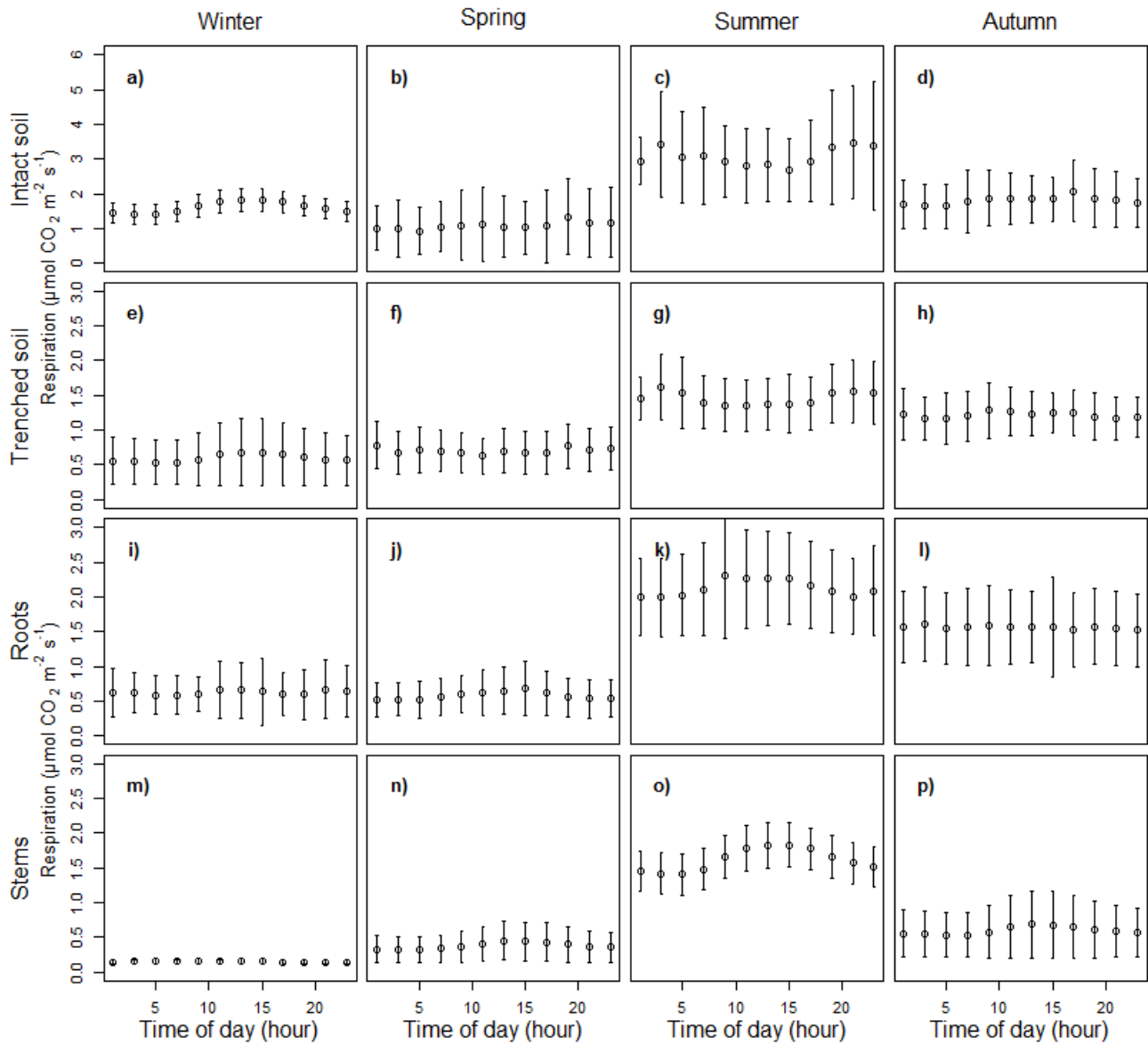
R_{soil}.

908

909 **Figure 3:** R_{soil} (solid lines) throughout the year measured by the automated closed-chambers and

910 soil temperature at 5 cm depth (dashed line). The black solid lines show the R_{soil} for the four plots

911 with intact soil and the red solid lines show R_{soil} for the two plots with trenched soil. The lines have

912 been smoothed to show a running five day average.

42
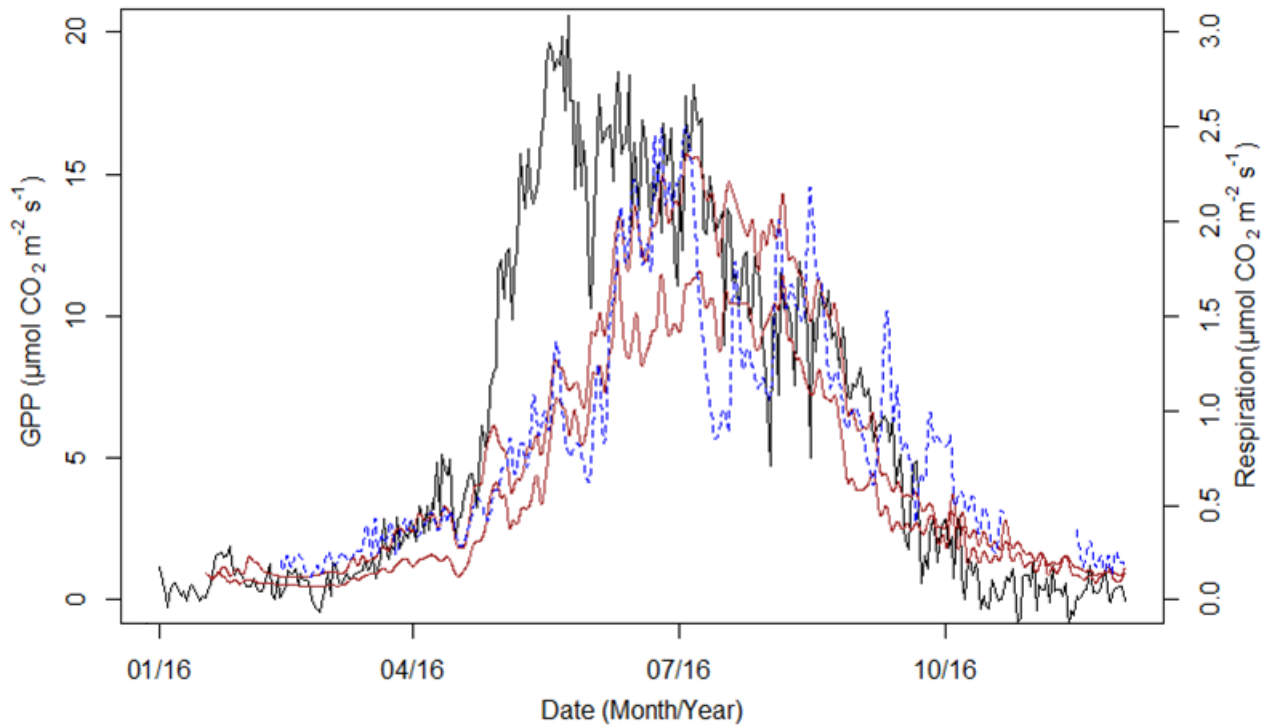
913

914 **Figure 4:** Mean daily GPP (black line, left y-axis) and R_{stem} (the red lines, right y-axis) throughout

915 the year. For R_{stem} both plots are shown. The blue dashed line shows the mean daily R_{soil} for the

916 intact soil plots measured by the automated closed-chambers. R_{soil} have been multiplied with 0.45 to

917 fit the right respiration scale.

918

Figure 5: Seasonally averaged diel patterns of R_{soil} for the intact and trenched soil, R_{root} and R_{stem}

measured by the automated closed-chambers for each of the four seasons. Error bars show standard

deviation. The seasons of winter, spring, summer and autumn are shown in the four columns from

left to right, respectively. The four rows from top to bottom show R_{soil} from intact soil, R_{soil} from

trenched soil, R_{root} and R_{stem}, respectively. R_{soil} is shown on a soil surface area basis, while R_{root} and

R_{stem} are shown on root surface area and stem surface area basis, respectively.
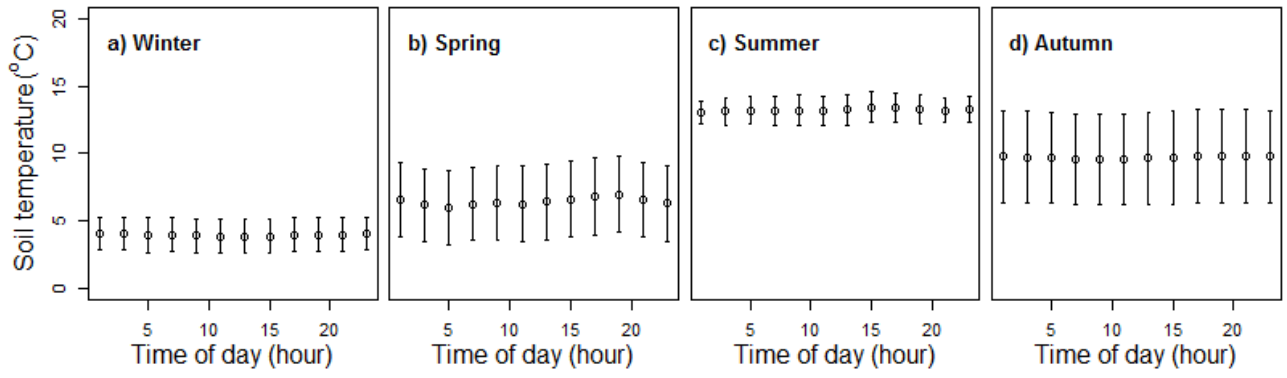
Figure 6: Seasonally averaged diel pattern of soil temperature (± standard deviation) at 5 cm depth measured by soil thermometers installed close to the automated chambers for winter (a), spring (b), summer (c) and autumn (d).